

# Chargeless spin current for switching and coupling of domain walls in magnetic nanowires

Chenglong Jia<sup>1,2\*</sup> and Jamal Berakdar<sup>2†</sup>

<sup>1</sup>*Key Laboratory for Magnetism and Magnetic Materials of the Ministry of Education, Lanzhou University, Lanzhou 730000, China*

<sup>2</sup>*Institut für Physik, Martin-Luther Universität Halle-Wittenberg, 06099 Halle (Saale), Germany*

## Abstract

The demonstration of the generation and control of a pure spin current (without net charge flow) by electric fields and/or temperature gradient has been an essential leap in the quest for low-power consumption electronics. The key issue of whether and how such a current can be utilized to drive and control information stored in magnetic domain walls (DWs) is still outstanding and is addressed here. We demonstrate that pure spin current acts on DWs in a magnetic stripe with an effective spin-transfer torque resulting in a mutual DWs separation dynamics and picosecond magnetization reversal. In addition, long-range ( $\sim$  mm) antiferromagnetic DWs coupling emerges. If one DW is pinned by geometric constriction, the spin current induces a dynamical spin orbital interaction that triggers an internal electric field determined by  $\mathbf{E} \sim \hat{e}_x \cdot (\mathbf{n}_1 \times \mathbf{n}_2)$  where  $\mathbf{n}_{1/2}$  are the effective DWs orientations and  $\hat{e}_x$  is their spatial separation vector. This leads to charge accumulation or persistent electric current in the wire. As DWs are routinely realizable and tuneable, the predicted effects bear genuine potential for power-saving spintronics devices.

*Introduction.* Generally, the interaction between charge currents and localized magnetic textures, e.g. domain walls (DWs), has attracted intense research as a paradigm for the interplay of charge and spin degrees of freedom, but also due to novel spintronic applications [1–3]. For instance, concepts based on magnetism being controlled by currents/current-induced torques (e.g., racetrack memory) are discussed as a yet new branch in the evolution of functionalities of spintronic devices [4–6]. In general, current-induced magnetization dynamics can be understood by means of the Landau-Lifshitz-Gibert equation (LLG) [7, 8]. Within this phenomenological description, two additional contributions to the torques may arise that stem from the spatially nonuniform magnetization [9, 10]. 1) An adiabatic spin-transfer torques (STT): in this case the carriers’ spins follow adiabatically the direction of the local magnetization; and 2) a nonadiabatic contribution that gains importance when the carriers wave length is comparable to the spatial extension of the non-collinear region. Thus, theoretically the spin-polarized, charged current-induced DW dynamics is fairly well understood. For applications, however, obstacles have to be circumvented that are associated by the required high charge current density entailing high energy consumption and dissipation.

As shown below, a surprisingly effective solution to these problems is achieved by going in a qualitatively novel direction and utilizing a pure carrier spin current, i.e. a flow of electron spin angular momentum. That such a spin current can be generated in a versatile and energy-effective way is evidenced by an impressive series of recent discoveries: E.g., an open circuit spin currents can be generated by a temperature gradient in a spin-Seebeck effect (SSE) geometry [11–14], or due to spin-Hall effect [15], or by means of ferromagnetic resonance [16]. These findings open the way for spintronic devices controlled by spin flow with the advantage of energy-consumption reduction [17]. The issue of how a long-lived *pure* carrier spin current can be utilized to steer magnetic textures (DWs) is obviously of a critical importance and has not yet been addressed, to the best of our knowledge. In this Letter, we show that in a magnetic nanowire with double DWs (cf. Fig.1a), interferences due to spin-dependent transmissions and reflections of the spin current give rise to an indirect long-range antiferromagnetic coupling between DWs. An *intrinsic* electric field related to the DWs configuration with a broken mirror symmetry is predicted,

$$\mathbf{E} \sim \hat{e}_x \cdot (\mathbf{n}_1 \times \mathbf{n}_2) \tag{1}$$

where  $\mathbf{n}_1$  and  $\mathbf{n}_2$  denote the directions of DWs polarization, respectively. By pinning one of the DWs at a constriction, the second DW is found to possess an ultrafast ( $\sim ps$ ) magnetic reversal and inter-domain wall displacement, evidencing that indeed spin current is a qualitatively new tool for spin-dynamics control.

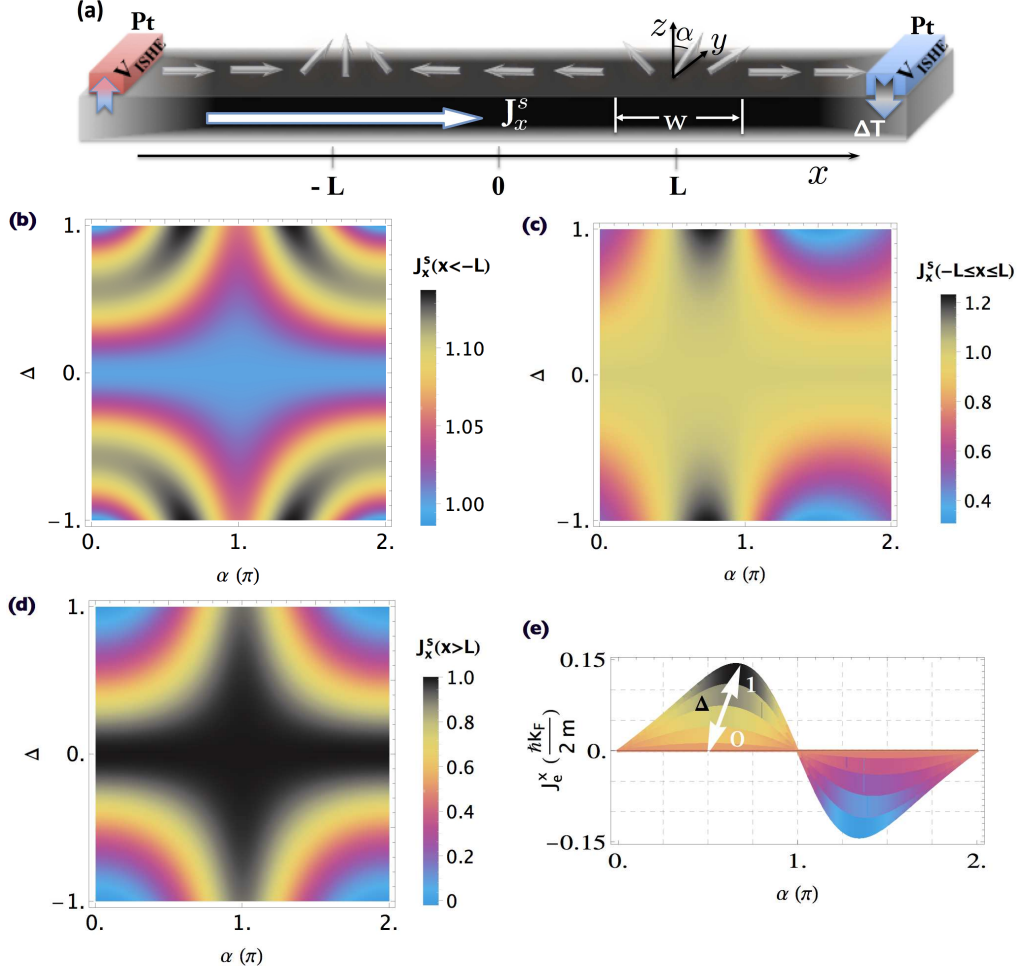


FIG. 1. (a) A ferromagnetic wire containing double domain walls subject to a spin current  $\mathbf{J}_x^s$ , which can be induced by the spin injection and/or spin pumping due to a mismatch of spin electrochemical potential with the Pt strips deposited on the sample, e.g., through the inverse spin-Hall effect (ISHE) or the longitudinal SSE. The magnetization profile is as shown schematically (thick arrows).  $\pm L$  and  $\alpha$  are, respectively, the DWs positions and orientation with respect to the  $xz$ -plane.  $w$  is the DW width. (b-c) Inhomogeneous spin current in the wire. (e) The magnetic scattering induced charge current with  $C_2$ -symmetry.  $\Delta$  is the effective spin-current scattering strength.

*Model.* The system under consideration is illustrated in Fig.1a: a ferromagnetic (FM) wire with a magnetization profile exhibiting two DWs, down which a spin current,  $\mathbf{J}_x^s$ , is passed. The two DWs have the same extension  $w$  and are separated by the distance  $2L$ . Their profile  $\mathbf{M}(x) = M_0 \mathbf{n}(x)$  is parameterized by the angles  $\alpha(x)$  and  $\varphi(x)$ , i.e.,  $n_x = \cos \varphi$ ,  $n_y = \sin \alpha \sin \varphi$ , and  $n_z = \cos \alpha \sin \varphi$ , where  $\varphi(x) = \arccos \left[ \tanh \frac{x+L}{w} \right] + \arccos \left[ \tanh \frac{x-L}{w} \right]$ . Without loss of generality, we set  $\alpha(-L) = \alpha_1 = 0$  at the first wall and  $\alpha(L) = \alpha_2 = \alpha$  around the second. The interaction between the delocalized electronic states with spin  $\sigma$  and the (classical) localized moments forming the DWs are modeled by the “ $s$ - $d$ ” Hamiltonian [9, 18] ( $g$  is a local exchange coupling strength)

$$H_{sd} = g \mathbf{M}(x) \cdot \boldsymbol{\sigma}. \quad (2)$$

Independent of the different underlying mechanisms for generating the spin current density,  $\mathbf{j}_\mu^s(k)$ , we can describe it with chargeless eigenstates  $\psi_B(x)$  [19],

$$\psi_B(x) = \frac{1}{2} \left[ e^{ikx} \begin{pmatrix} 1 \\ 1 \end{pmatrix} + e^{-ikx} \begin{pmatrix} e^{i\theta} \\ e^{-i\theta} \end{pmatrix} \right]. \quad (3)$$

The first term generates a spin current along the wire;  $\theta \in [0, 2\pi]$  in the second term accounts for residual spin precession and diffusion. With this, one obtains a finite spin expectation value along the wire only, i.e.  $\langle \sigma_x \rangle \neq 0$  but  $\langle \sigma_y \rangle = 0$ . The  $x$  expectation value of the charge current  $\mathbf{j}^e(k) = \frac{i\hbar}{2m} [(\nabla \psi^\dagger(x))\psi(x) - \psi^\dagger(x)\nabla \psi(x)]$  vanishes, i.e.  $j_x^e(k) \equiv 0$  (here  $m$  is the effective mass). In contrast, for the spin current  $\mathbf{j}_\mu^s(k) = \frac{i\hbar}{2m} [(\nabla \psi^\dagger(x))\sigma_\mu \psi(x) - \psi^\dagger(x)\sigma_\mu \nabla \psi(x)]$  one finds  $J_y^s = \oint j_y^s d\theta / 2\pi = 0$ , whereas  $J_x^s = J_0^s = \hbar k / 2m$ , respectively. These properties are particularly in line with experimental observations in the SSE geometry [11–14].

The primary quantity on which we focus our interest will be the spin-current transmission/reflection mediated DWs coupling. If the internal structure of  $\mathbf{M}(x)$  varies on a scale larger than the electron wavelength at the Fermi surface  $k_F$ , then the spin of conduction electrons follows the smoothly varying nonlinear magnetic texture. One can then unitarily transform to align locally with  $\mathbf{M}$ , which introduces a nontrivial Berry curvature field and gives rise to the “spin motive force” [20–22]. On the other hand, for sharp DWs, i.e. if  $\lambda_F = 2\pi/k_F \gtrsim w$  (as realized in magnetic semiconductor-based structures), DW scatters strongly the carriers acting in effect as  $\mathbf{M}(x) = \mathbf{M}_0 \delta(x)$  [18, 23]. Consequently, the scattering

spinor wave function in the presence of double DWs can be expressed as,

$$\psi'_s(x) = \begin{cases} \frac{e^{ikx}}{2} (1) + \frac{e^{-ikx}}{2} (r'_1) + \frac{e^{-ikx}}{2} (t'_1 e^{i\theta}) & x < -L, \\ \frac{e^{ikx}}{2} (t_2) + \frac{e^{-ikx}}{2} (r'_2) + \frac{e^{-ikx}}{2} (t'_2 e^{i\theta}) + \frac{e^{ikx}}{2} (r'_2 e^{-i\theta}), & |x| \leq L, \\ \frac{e^{ikx}}{2} (t_1) + \frac{e^{-ikx}}{2} (e^{i\theta}) + \frac{e^{ikx}}{2} (r_1 e^{-i\theta}) & x > L. \end{cases} \quad (4)$$

The complex coefficients  $t_i(t'_i)$  and  $r_i(r'_i)$  describe the spin reflection and transmission with reference to the original spin and spin-flip channels, and they can be analytically determined by the wave function continuity at  $x = \pm L$ .

*Magnetoelectric effect.* At first, let us inspect the case of a small Fermi wave vector  $k_F$ ; or  $k_FL \ll 1$ . We have then  $t'_1 = t_1^* = \frac{i}{i+\Delta}$  and  $r'_1 = r_1^* = -\frac{\Delta}{i+\Delta}$  with  $\Delta = kw \times \frac{gM_0}{\hbar^2 k^2 / 2m}$  being an effective spin-current scattering strength. We readily infer that the spin current is not influenced by the detailed configuration of two DWs and scatters equivalently from a composite magnetic cluster, setting such a collection of localized moments in a precessional and displacement motion as discussed in Ref.[19]. For a intermediate Fermi wave vector and/or a sufficiently large distance between the DWs, such that  $k_FL \geq 1$  whereas  $k_F w \ll 1$ , the spin-dependent interferences due to scattering from DWs result in a long-range interaction of DWs. Here the spin coherence is necessary which seems to be realizable ( $L_s \sim mm$ ) via thermal [15, 24] or dynamical [16] approaches. Physically, the scattering leads to a redistribution of the spin electrochemical potential along the wire, resulting in a non-conserved spin current. Its density is inhomogeneous in three different region (cf. Fig.1(b-d)), which can be imaged electrically by means of the inverse spin Hall effect, e.g. by measuring a voltage build up in a Pt strip deposited on the sample perpendicular to the transport of spin current. Importantly, quite different to a short pseudocircuit in the charge channels in the case of single magnetic scattering [19], now we have a spin-current-induced persistent electric current

$$\langle j_x^e \rangle = -\frac{\hbar k}{2m} \frac{32\Delta^2 \sin \alpha \sin(4kL)}{[\Delta^4 - 4\Delta^2 \cos \alpha - (\Delta^4 + 4\Delta^2 + 8) \cos(4kL)]^2 + 16(\Delta^2 + 2)^2 \sin^2(4kL)} \quad (5)$$

after integrating out the residual spin precession and diffusion over  $\theta$  (see also in Fig.1e). Phenomenologically, the DW has been predicted to behave at low energy as a magnetic impurity [25], and consequently we have now two localized magnetic moments indirectly

coupled through the carrier-mediated exchange interaction. Given  $\alpha \neq 0$  (or  $\pi$ ), from the symmetry point of view, the DWs configurations lose the mirror symmetry with respect to the  $zx$  plane, which points to an antisymmetric Dzyaloshinsky-Moriya interaction along the wire [26]. In fact, the  $E_x$  component of an electric field is allowed by symmetry, as discussed for multiferroic transition metal oxides [27]. Qualitatively, such an internal electric field is expressible by the vector products of DWs,  $E_x \sim \hat{e}_x \cdot (\mathbf{n}_1 \times \mathbf{n}_2)$  that would induce charge accumulation and/or electric current with  $C_2$  symmetry, as demonstrated in Fig.1e. Note that the angular-dependence of the induced charge current rules out a possible  $C_{2v}$  planar Nernst effect [28, 29]. Thus, we can identify the rearrangements of DWs upon the encounter with the spin current having a defined direction as the underlying mechanism for the emergence of the electric field along the wire. This is insofar important as, beside the spin-current-induced macroscopic magnetoelectric effect, the setup in Fig.1a possesses multiple functionalities: it can be a thermally driven electric generator [30] provided that two DWs are mechanically pinned in non-coplanar manner.

*Magnetic dynamics.* The interference of incoming and reflected waves are expected to result in current-induced torques acting on the walls [7, 8]. Subsequently, we study STT and DWs dynamics. For definiteness, let's assume that one of the DWs (say left) at  $x = -L$  is pinned, and concentrate on the effect of spin current on the right DW with initial

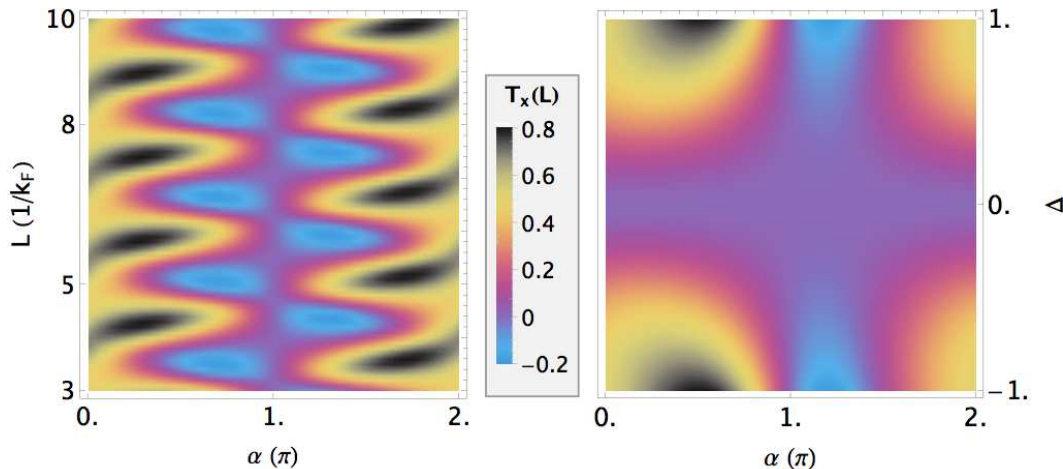


FIG. 2. The  $\hat{x}$  component of the spin-current-induced STT  $\mathbf{T}_x(L)$  around the right domain wall as functions of the polar angle  $\alpha$  and (left) the DWs distance  $L$  with  $\Delta = 0.72$ , or (right) the effective spin-current scattering strength  $\Delta$  with  $k_FL = 3$ , respectively.

magnetization  $\mathbf{M}$  perpendicularly polarized at  $x = L$  (i.e.,  $\alpha(t = 0) = 0$ ). The spin current acts on the right DW with a torque  $\mathbf{T}_\mu(x)$  that follows from the jump in the spin current at the point  $x$ , or equivalently, within our model, from the nonequilibrium spin density  $s_\mu(x)$  accumulation

$$\mathbf{T}_\mu(x) = -\frac{gM_0}{\hbar}[\mathbf{n} \times \mathbf{s}(x)]_\mu, \quad (6)$$

where  $\mathbf{n}$  is the unit vector along  $\mathbf{M}$ , and the spin density we obtain from  $s_\mu(x) = \psi_s^{\prime\dagger}(x)\sigma_\mu\psi_s'(x)$ . Upon scattering, the spin current carried by Eq.(3) is modified, nonzero  $J_y^s$  and  $J_z^s$  emerge inhomogeneously in three different regions:  $x < -L$ ,  $|x| \leq L$ , and  $x > L$ . The calculated STT on the right DW is shown in Fig.2. Clearly, the STT depends on the sign of the current and periodically on the DWs relative angle  $\alpha$  and distance  $2L$ . The mag-

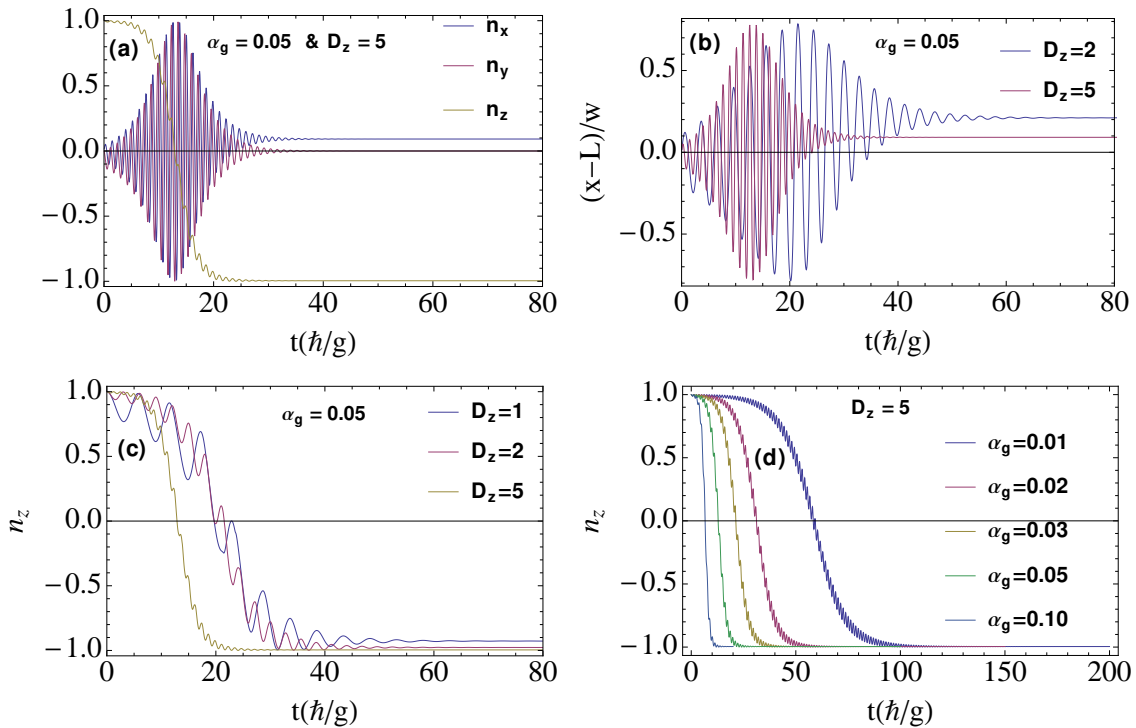


FIG. 3. The magnetization dynamics of the right domain wall: (a) Magnetic reversal. (b) Oscillation and displacement of the DW. The spin-current-induced magnetic reversal with respect to the transition from parallel to anti-parallel DWs configuration for different (c) perpendicular anisotropy  $D_z$  (in scale of  $g$ ) and (d) Gilbert damping  $\alpha_g$ . For the numerical calculations we take the spin-current scattering strength  $\Delta = 0.72$ .

netization dynamics are then modelled with the modified Landau-Lifshitz-Geilbert (LLG) equation [8, 31]

$$\frac{\partial \mathbf{n}}{\partial t} = \frac{D_z}{\hbar}[\mathbf{n} \times \hat{e}_z] + a_g \mathbf{n} \times \frac{\partial \mathbf{n}}{\partial t} - \frac{g}{\hbar}[\mathbf{n} \times \mathbf{s}(L)] \quad (7)$$

where  $a_g$  is the Gilbert damping parameter and  $D_z$  is the perpendicular anisotropy energy [32, 33]. It should be noted that the temperature effect can be included as a stochastic field contributing to the effective magnetic field in LLG equation, however, it is shown that at low temperature, thermal fluctuations do not alter qualitatively the LLG dynamics [34]. With an initial parallel configuration of the DWs, we calculated the time dependence of the right DW magnetization shown in Fig.3 [35]. As concluded from the figures, the right DW is set in oscillating motion immediately when subjected to the spin current, which is different from the continuous displacements of a single localized magnetic structure [19, 36]. Furthermore, in spite of the large deviation of the spin density from the localized magnetization, the non-adiabatic torque [9] is absent in our case and the DW motion is terminated with magnetic reversal and small center shift of the wall along the wire. During its propagation, STT causes DW distortion developing an out-of-plane component of the magnetization, which exhibits a fast oscillation mode exacerbated by the anisotropically damped motion in the  $\hat{z}$  direction (c.f. Fig.3(b-c)). The magnetization switching time can be shown to be mainly determined by  $D_z/\alpha_g$ . Even a small spin-current scattering strength,  $\Delta = 0.01$  is found to give a magnetic reversal because of a substantial reduction of the critical current due to the perpendicular anisotropy [37].

*Discussion.* On the scale of the carriers motion DW may be considered nearly static. Let us assume that two DWs are located at their potential minima as local spins,  $\mathbf{M}_1$  and  $\mathbf{M}_2$ . The spin-current channel naturally gives rise to an effective multi-orbital electron hopping between the spins  $\mathbf{M}_i$ . The Hamiltonian describing it, can take a simple form  $H_t = -t \sum_{ia,jb} c_{jb}^\dagger c_{ia}$  with  $t$  being the amplitude of hopping from the orbital  $a$  on the site  $i$  to the orbital  $b$  on the site  $j$ . Given that the time of the magnetic reversal ( $t \sim 10\hbar g^{-1}$ ) is much longer than the hopping time ( $\sim \hbar g^{-1}$ ), to a lowest order we obtain an effective antiferromagnetic interaction between DWs [38],

$$H_S = \frac{t^2}{g/4}(\mathbf{n}_1 \cdot \mathbf{n}_2 + 1). \quad (8)$$

Considering the macroscopic spin coherence length over  $mm$ , one has thus a long-range spin-current induced antiferromagnetic coupling, resulting in anti-parallel configuration of

two DWs in equilibrium state, which is consistent with the long-time behavior of magnetic dynamics (cf. Fig.3). Furthermore, there should be a dynamic magnetoelectric coupling during the distorted DWs oscillations as well [20, 21], which allows possibly for a dynamical electric control of DWs structures by voltage pulse.

*Conclusions and outlook.* Pure spin current interaction with magnetic DWs results in 1.) long-range antiferromagnetic DWs coupling, and 2.) in STT-induced picosecond magnetic reversal for DWs with initially parallel polarizations. 3.) For two DWs pinned in a non-coplanar configuration, an internal magnetoelectric effect with  $C_2$  symmetry is predicted. Linking theory to experiment we note: favorable materials satisfy  $w < \lambda_F < L$  predestinating dilute magnetic semiconductors [39]. E.g., for GaMnAs the domain wall width,  $w$  varies within 4 – 12 nm [42] and the hole concentration is around  $10^{18} - 10^{20} \text{ cm}^{-3}$  [43]. We estimate  $k_F = \pi\rho_{1D} = S\pi \times 10^{-2} \text{ nm}^{-1}$ , where  $\rho_{1D}$  is the linear hole density related to the bulk density by  $\rho_{1D} = \rho_{3D}S$  and  $S$  is the cross section (in unit of  $\text{nm}^2$ ) and  $\rho_{3D} = 10^{19} \text{ cm}^{-3}$ . Thus, the area of the cross section is roughly  $\sim 10 \text{ nm}^2$ . The local exchange coupling  $g$  in GaMnAs deduced from experiments [44, 45] is about 0.02 – 1 meV; the perpendicular anisotropy energy density varies (also with temperature) in 0.01 – 0.05 meV/nm<sup>3</sup> [42, 45, 46]. The damping coefficient  $\alpha_G$  as deduced from the domain wall mobility measurement [46, 47] is  $\alpha_G = 0.25 \pm 0.05$  (from ferromagnetic resonance  $\alpha_G \approx 0.01$  [48, 49]). In GaMnAs pure spin-current may be delivered by SSE [13]. Thus, all parameters in the present theory and simulations are experimentally accessible. The theory is also applicable to open circuit dynamics in magnetic textures in insulators or molecules coupled to a spin current, e.g. LaY<sub>2</sub>Fe<sub>5</sub>O<sub>12</sub>/Fe [12], or FM/Mn<sub>12</sub>/Fe [50]. Hence, the present approach is versatile and allows to uncover spin-current-induced effects such as magnetoelectric effect and ultrafast DW reversal pointing so to new possible concepts for efficient spintronic devices.

This work was supported by the National Basic Research Program of China (No. 2012CB933101), the German Research Foundation (No. SFB 762, and BE 2161/5-1), the National Natural Science Foundation of China (No. 11104123), the Program for Changjiang Scholars and Innovative Research Team in University (No. IRT1251), and the Fundamental Research Funds for the Central Universities (No. 2022013zrct01/2022013zr0017). J.B. acknowledges useful discussions with S.S.P. Parkin on the experimental aspects.

---

\* cljia@lzu.edu.cn

† jamal.berakdar@physik.uni-halle.de

- [1] A. Thiaville and Y. Nakatani, *Spin Dynamics in Confined Magnetic Structures III*, Topics in Applied Physics Vol. **101** (Springer-Verlag, Berlin, 2006).
- [2] G. S. D. Beach, M. Tsoi, and J. L. Erskine, *J. Magnetism and Magnetic Materials* **320**, 1272 (2008).
- [3] A. A. Khajetoorians, B. Baxevanis, C. Hubner, T. Schlenk, S. Krause, T. O. Wehling, S. Lounis, A. Lichtenstein, D. Pfannkuche, J. Wiebe, and R. Wiesendanger, *Science* **339**, 55 (2013).
- [4] S. S. P. Parkin, M. Hayashi, and L. Thomas, *Science* **320**, 190 (2008).
- [5] L. Thomas, R. Moriya, C. Rettner, and S. S. Parkin, *Science* **330**, 1810 (2010).
- [6] G. E. W. Bauer, E. Saitoh, and B. J. van Wees, *Nature Materials* **11**, 391 (2012).
- [7] D. C. Ralph and M. D. Stiles, *J. Mag. and Magnetic Materials* **320**, 1190 (2008).
- [8] A. Brataas, A. D. Kent, and H. Ohno, *Nature Materials* **11**, 372 (2012).
- [9] S. Zhang and Z. Li, *Phys. Rev. Lett.* **93**, 127204 (2004).
- [10] G. Tatara and H. Kohno, *Phys. Rev. Lett.* **92**, 086601 (2004).
- [11] K. Uchida, S. Takahashi, K. Harii, J. Ieda, W. Koshibae, K. Ando, S. Maekawa, E. Saitoh, *Nature* **455**, 778 (2008).
- [12] K. Uchida, J. Xiao, H. Adachi, J. Ohe, S. Takahashi, J. Ieda, T. Ota, Y. Kajiwara, H. Umezawa, H. Ka-wai, G. E.W. Bauer, S. Maekawa and E. Saitoh, *Nature Mat.* **9**, 894 (2010).
- [13] C. M. Jaworski, J. Yang, S. Mack, D. D. Awschalom, J. P. Heremans and R. C. Myers, *Nature Mat.* **9**, 898 (2010).
- [14] C. M. Jaworski, R. C. Myers, E. Johnston-Halperin, and J. P. Heremans, *Nature* **487**, 210 (2012).
- [15] Y. Kajiwara, K. Harii, S. Takahashi, J. Ohe, K. Uchida, M. Mizuguchi, H. Umezawa, H. Kawai, K. Ando, and K. Takanashi, *Nature* **464**, 262 (2010).
- [16] E. Shikoh, K. Ando, K. Kubo, E. Saitoh, T. Shinjo, and M. Shiraishi, *Phys. Rev. Lett.* **110**, 127201 (2013).
- [17] S. Maekawa, Sergio O. Valenzuela, E. Saitoh, and T. Kimura, *Spin Current* (Oxford University

- Press, 2012).
- [18] V.K. Dugaev, J. Berakdar, and J. Barnaś, Phys. Rev. Lett. **96**, 047208 (2006).
  - [19] C.L. Jia and J. Berakdar, Phys. Rev. B **83**, 180401(R) (2011).
  - [20] S. Barnes and S. Maekawa, Phys. Rev. Lett. **98**, 246601 (2007).
  - [21] S. Yang, G. Beach, C. Knutson, D. Xiao, Q. Niu, M. Tsoi, and J. Erskine, Phys. Rev. Lett. **102**, 067201 (2009).
  - [22] T. Schulz, R. Ritz, A. Bauer, M. Halder, M. Wagner, C. Franz, C. Pfleiderer, K. Everschor, M. Garst, and A. Rosch, Nature Physics **8**, 301 (2012).
  - [23] V. Dugaev, V. Vieira, P. Sacramento, J. Barnas, M. Arajo, and J. Berakdar, Phys. Rev. B **74**, 054403 (2006).
  - [24] K. Uchida, T. Ota, H. Adachi, J. Xiao, T. Nonaka, Y. Kajiwara, G. Bauer, S. Maekawa, and E. Saitoh, J. Appl. Phys. **111**, 103903 (2012).
  - [25] E. Saitoh, H. Miyajima, T. Yamaoka, and G. Tatara, Nature **432**, 203 (2004).
  - [26] K. Yosida, *Theory of Magnetism*, (Springer-Verlag, Berlin Heidelberg, 1996).
  - [27] C.L. Jia, S. Onoda, N. Nagaosa, and J.H. Han, Phys. Rev. B **74**, 224444 (2006); Phys. Rev. B **76**, 144424 (2007).
  - [28] Yong Pu, E. Johnston-Halperin, D. D. Awschalom, and Jing Shi, Phys. Rev. Lett. **97**, 036601 (2006).
  - [29] A. D. Avery, M. R. Pufall, and B. L. Zink, Phys. Rev. Lett. **109**, 196602 (2012).
  - [30] G. E. W. Bauer, S. Bretzel, A. Brataas, and Y. Tserkovnyak, Phys. Rev. B **81**, 024427 (2010).
  - [31] Y. B. Bazaliy, B. A. Jones, and S.-C. Zhang, Phys. Rev. B **57**, R3213 (1998).
  - [32] I. M. Miron, T. Moore, H. Szambolics, L. D. Buda-Prejbeanu, S. Auffret, B. Rodmacq, S. Pizzini, J. Vogel, M. Bonfim, and A. Schuhl, Nature Materials **10**, 419 (2011).
  - [33] J. Curiale, A. Lematre, C. Ulysse, G. Faini, and V. Jeudy, Phys. Rev. Lett. **108**, 076604 (2012).
  - [34] A. Sukhov, J. Berakdar, Phys. Rev. Lett. **102**, 057204 (2009).
  - [35] The calculations were performed self-consistently while taking into account simultaneously the development of the out-of-plane components of the second DW, *i.e.*, the polar angle  $\alpha$  is relaxed to vary with  $t$  during the LLG dynamics.
  - [36] Z. Li and S. Zhang, Phys. Rev. Lett. **92**, 207203 (2004).
  - [37] S.-W. Jung, W. Kim, T.-D. Lee, K.-J. Lee, and H.-W. Lee, Appl. Phys. Lett. **92**, 202508

- (2008).
- [38] M. Mostovoy, K. Nomura, and N. Nagaosa, Phys. Rev. Lett. **106**, 047204 (2011).
- [39] For metals, DW spatial variation is larger than  $2\pi/k_F$ . Scattering is treated perturbatively using the Green's function constructed from Eq.(3) (cf. Refs. [40] and [41]). Effects of non-adiabatic transfer torque, the so called  $\beta$  term emerge and may induce a steady state DW motion [9, 33].
- [40] N. Sedlmayr, V. K. Dugaev, and J. Berakdar, Phys. Rev. B **79**, 174422 (2009); N. Sedlmayr, V. K. Dugaev, M. Inglot, and J. Berakdar, Phys. Status Solidi RRL **5**, 450 (2011).
- [41] V. K. Dugaev, J. Barnas and J. Berakdar, J. Phys. A **36**, 9263 (2003).
- [42] C. Gourdon, A. Dourlat, V. Jeudy, K. Khazen, H. von Bardeleben, L. Thevenard, and A. Lematre, Phys. Rev. B **76**, 241301(R) (2007).
- [43] F. Matsukura, H. Ohno, A. Shen, and Y. Sugawara, Phys. Rev. B **57**, R2037 (1998).
- [44] S. T. B. Goennenwein, T. Graf, T. Wassner, M. S. Brandt, M. Stutzmann, J. B. Philipp, R. Gross, M. Krieger, K. Zrn, P. Ziemann, A. Koeder, S. Frank, W. Schoch, and A. Waag, Appl. Phys. Lett. **82**, 730 (2003).
- [45] S. Haghgoo, M. Cubukcu, H. J. von Bardeleben, L. Thevenard, A. Lemaitre, and C. Gourdon, Phys. Rev. B **82**, 041301(R) (2010).
- [46] A. Dourlat, V. Jeudy, A. Lematre, and C. Gourdon, Phys. Rev. B **78**, 161303(R) (2008).
- [47] J.-P. Adam, N. Vernier, J. Ferr, A. Thiaville, V. Jeudy, A. Lematre, L. Thevenard, and G. Faini, Phys. Rev. B **80**, 193204 (2009).
- [48] K. Khazen, H. J. von Bardeleben, M. Cubukcu, J. L. Cantin, V. Novak, K. Olejnik, M. Cukr, L. Thevenard, and A. Lematre, Phys. Rev. B **78**, 195210 (2008).
- [49] M. Cubukcu, H. J. von Bardeleben, K. Khazen, J. L. Cantin, O. Mauguin, L. Largeau, and A. Lematre, Phys. Rev. B **81**, 041202 (2010).
- [50] One FM could be a heated, unbiased STM tip. Other FM serves as a substrate for Mn<sub>12</sub> molecules [51, 52]. The total spin and diameter of Mn<sub>12</sub> are  $M_0 = 10$  and  $w = 3$  nm; the exchange coupling is  $gM_0 = 1$  meV [53], and  $\alpha_G \approx 0.17$  and  $\hbar/g \approx 6.6 \times 10^{-12}$ s. These parameters are in the range of our simulations.
- [51] H. B. Heersche, Z. de Groot, J. A. Folk, H. Van der Zant, C. Romeike, M. R. Wegewijs, L. Zobbi, D. Barreca, E. Tondello, and A. Cornia, Phys. Rev. Lett. **96**, 206801 (2006).
- [52] M.-H. Jo, J. E. Grose, K. Baheti, M. M. Deshmukh, J. J. Sokol, E. M. Rumberger, D. N.

- Hendrickson, J. R. Long, H. Park, and D. C. Ralph, *Nano Lett.* **6**, 2014 (2006).
- [53] R.-Q. Wang, L. Sheng, R. Shen, B. Wang, and D. Y. Xing, *Phys. Rev. Lett.* **105**, 057202 (2010).